Available online at www.elixirpublishers.com (Elixir International Journal)

Vibrational Spectroscopy

Elixir Vib. Spec. 92 (2016) 38632-38639

ISSN: 2229-712X

Molecular Structure, Vibrational Spectroscopic, Natural Bond Orbital Analysis, Frontier Molecular Orbital Analysis and Thermodynamic Properties of 3-Hydroxynaphthalene-2-carboxylic acid

B. Raja[1], V. Balachandran[2*], B. Narayana[3] and B.Revathi[2]
[1]Department of Physics, Government Arts College, Kulithalai 639120, Karur, India.
[2]Department of Physics, A. A. Government Arts College, Musiri 621211, India.
[3]Department of Studies in Chemistry, Mangalore University, Mangalagangotri 574 199, India.

ARTICLE INFO

Article history:
Received: 9 January 2016;
Received in revised form:
25 February 2016;
Accepted: 1 March 2016;

Keywords
3-Hydroxynaphthalene-2-carboxylic acid,
Vibrational Spectra,
Mulliken Atomic Charges,
NBO,
HOMO-LUMO Energy Gap
MEP Surface.

ABSTRACT

The understanding of optimized molecular geometry, vibrational analysis of the heterocyclic organic compounds plays a vital role in the process of drug discovery. The present work provides geometrical parameters, vibrational assignments for pharmaceutical intermediate 3-hydroxynaphthalene-2-carboxylic acid (3HN2CA). Moreover, the present study aims to illustrate how intermolecular interactions appear within the molecule on account of HOMO-LUMO studies. In addition to these, Mullikan's Atomic charges associated with each atom are also reported. Entire vibrational, geometrical parameters, Mullikan's Atomic charges and HOMO-LUMO Energy gap of 3HN2CA were predicted with the aid of B3LYP level of theory with cc/PVDZ and 6-31+G(d) basis sets on a quantum chemical software Gaussian 09W. In view of visual inspection, 60 normal modes of vibrations contributed to 3HN2CA were found out. Furthermore, the molecular orbital calculations such as natural bond orbital's (NBOs) and Mapped molecular electrostatic potential (MEP) surfaces were also performed with the same level of DFT. The thermal flexibility of molecule in associated with vibrational temperature was also illustrated on the basis of correlation graphs. The detailed interpretation of the vibrational spectra has been carried out with the aid of potential energy distribution (PED) results obtained quantum chemical calculations. The delocalization of electron density of various constituents of the molecule has been discussed with the aid of NBO analysis.

Introduction

The radical COOH has only a separate fleeting existence [1]. The acid dissociation constant of COOH has been measured using electron paramagnetic resonance spectroscopy [2]. The carboxyl group tends to dimerise to form oxalic acid. Deprotonation of carboxylic acids gives carboxylate anions; these are resonance stabilized, because the negative charge is delocalized over the two oxygen atoms, increasing the stability of the anion. Each of the carbon-oxygen bonds in the carboxylate anion has a partial double-bond character. Carboxylic acids are readily identified as such by infrared spectroscopy. They exhibit a sharp band associated with vibration of the C-O vibration bond ($\nu_{C=O}$) between 1680 and 1725 cm^{-1}. A characteristic $\nu_{O\text{-}H}$ band appears as a broad peak in the 2500 to 3000 cm^{-1} region[3]. By ^1H NMR spectrometry, the hydroxyl hydrogen appears in the 10–13 ppm region, although it is often either broadened or not observed owing to exchange with traces of water. Many carboxylic acids are produced industrially on a large scale. They are also pervasive in nature. Esters of fatty acids are the main components of lipids and polyamides of aminocarboxylic acids are the main components of proteins. Carboxylic acids are used in the production of polymers, pharmaceuticals, solvents, and food additives. Industrially important carboxylic acids include acetic acid (component of vinegar, precursor to solvents and coatings), acrylic and methacrylic acids (precursors to polymers, adhesives), adipic acid (polymers), citric acid (beverages), ethylenediaminetetraaceticacid(chelatingagent), fattyacids (coatings), maleicacid (polymers), propionic acid (food preservative), terephthalic acid (polymers).

To gain a better understanding of the performance and limits of DFT methods as a general approach to the vibrational problems of organic molecules, we calculated harmonic frequencies of 3-hydroxynaphthalene-2-carboxylicacid(3HN2CA by DFT method, and compared these results with observed fundamental vibrational frequencies. The aim of this work is to check the performance of B3LYP density functional force field for simulation of IR and Raman spectra of the title compound with the use of standard ccPVDZ and 6-31+G(d)basis sets.

Experimental Details

3HN2CA was provided by Lancaster Chemical Company, UK. Which is of spectroscopic grade and hence used for recording the spectra as such without any further purifications. The room temperature Fourier Transform infrared spectrum of 3HN2CA was measured in the 4000-450cm^{-1}

Tele: +91 9894253672
E-mail address: brsbala@rediffmail.com

region at a resolution of ± 1cm^{-1} using BRUKER IFS-66V FT-IR Spectrometer equipped with a KBR pellets were used in the spectral measurements. The FT-Raman spectrum was recorded on a BRUKER IFS-66V model interferometer equipped with an FRA -106 FT-Raman accessories in the 4000-100 cm^{-1} stokes region using the 1064nm line of an Nd: YAG laser for excitation operating at 200mW Power.

Computational details

Analysis of molecular geometry optimizations, energy, and vibrational frequencies was carried out with the Gaussian 09 software package [4] at the DFT (B3LYP) levels supplemented with the standard ccPVDZ and 6-31+G(d)basis sets. Cartesian representation of the theoretical force constants has been computed at optimized geometry. Vibrational Modes were assigned by means of visual inspection using the GAUSSVIEW [5] program. Data revealed that DFT calculations using a basis set incorporating polarized functions yielded results that are in better agreement with the experimental data. For the plots of simulated IR and Raman spectra, pure Lorentzian band shapes were used with a band width of ±1 cm^{-1}. Prediction of Raman intensities was carried out by the following procedure. The Raman activities (Si) calculated by the Gaussian 09 program were converted to relative Raman intensities (Ii) using the following relationship derived from the basic theory of scattering.

$$I_i = \frac{f(\nu_0 - \nu_i)^4 s_i}{\nu_i [1 - \exp(\frac{-hc\nu_i}{kt})]} \cdots \cdots \qquad (1)$$

where ν_0 is the exciting wave number (cm^{-1} units ν_i is the vibrational wave number of the ith normal mode, h, c and k are universal constant and f is a suitably chosen common normalization factor for all peak intensities.

Natural bond orbital analysis (NBO) was also performed by the Gaussian 09 W program at the B3LYP level of theory analysis transforms the canonical delocalized Hartree-Fork (HF) Molecular orbital's (MO) into localized MOs that are closely tied to chemical bonding concepts. This process involves sequential transformation of non-orthogonal Atomic orbital's (AOs) to the sets of Natural atomic orbital's (NAOs), Natural hybrid orbital's (NHOs) Natural bond orbital's (NBOs). The localized basis sets are completely described the wave functions in the most economic method, as electron density and other properties that are described by the minimum amount of filled NBO. The interaction between filled and anti-bonding (or) Rydberg orbital's represented the deviation of the molecule from the Lewis structure and be used as the measure of delocalization. This non-covalent bonding anti-bonding charge transfer interactions can be quantitatively described in terms of the second order perturbation interaction energy (E$^{(2)}$) [6-9].

Results and discussion

Molecular geometry

The molecular structure of a 3HN2CA along with numbering of atoms is shown in Fig. 1.

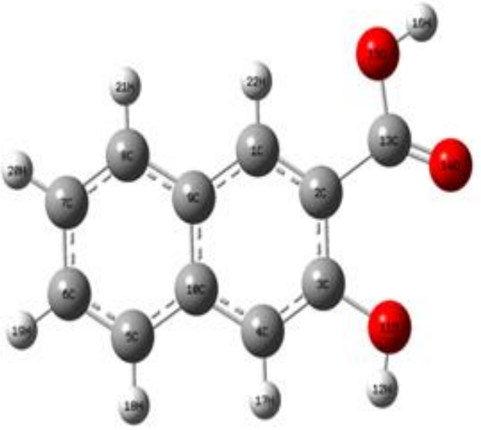

Fig 1. Optimized geometrical structure and atomic labeling of 3-hydroxynaphthalene-2-carboxylicacid

Table 1. Optimized geometrical parameters of 3-hydroxynaphthalene-2-carboxylicacid by B3LYP/ccPVDZ and B3LYP/6-31+G(d)

Parameters	Bond length		Parameters	Bond angle	
	B3LYP / ccPVDZ	B3LYP/ 6-31+G(d)		B3LYP / ccPVDZ	B3LYP / 6-31+G(d)
C1-C2	1.39	1.39	C2-C1-C9	122.57	122.60
C1-C9	1.42	1.41	C2-C1-H22	118.49	118.61
C1-H22	1.09	1.08	C9-C1-H22	118.94	118.79
C2-C3	1.44	1.44	C1-C2-3C	118.67	118.48
C2-C13	1.49	1.49	C1-C2-C13	119.91	119.88
C3-C4	1.38	1.38	C3-C2-C13	121.42	121.64
C3-O11	1.36	1.36	C2-C3-C4	119.68	119.92
C4-C10	1.42	1.42	C2-C3-O11	118.50	118.47
C4-H17	1.09	1.09	C4-C3-O11	121.82	121.61
C5-C6	1.38	1.38	C3-C4-C10	121.95	121.84
C5-C10	1.42	1.42	C3-C4-H17	119.14	119.29
C5-H18	1.09	1.09	C10-C4-H17	118.91	118.87
C6-C7	1.42	1.42	C6-C5-C10	120.65	120.62
C6-H19	1.09	1.09	C6-C5-H18	120.38	120.37
C7-C8	1.38	1.38	C10-C5-H18	118.97	119.02
C7-H20	1.09	1.09	C5-C6-C7	120.76	120.76
C8-C9	1.42	1.42	C5-C6-H19	119.78	119.78
C8-H21	1.09	1.09	C7-C6-H19	119.46	119.46
C9-C10	1.43	1.43	C6-C7-C8	119.43	119.95
O11-H12	0.97	0.97	C6-C7-H20	119.74	119.73
C13-O14	1.21	1.21	C8-C7-H20	120.33	120.32
C13-O15	1.37	1.37	C7-C8-C9	120.73	120.68
O15-H16	0.97	0.97	C7-C8-H21	120.58	120.57
			C9-C8-H21	118.69	118.76
			C1-C9-C8	122.23	122.16
			C1-C9-C10	118.44	118.47
			C8-C9-C10	119.34	119.37
			C4-C10-C5	122.70	122.68
			C4-C10-C9	118.70	118.69
			C5-C10-C9	118.60	118.63
			C3-O11-H12	108.07	109.05
			C2-C13-O14	126.89	126.95
			C2-C13-015	111.91	112.95
			O14-C13-015	121.20	120.91
			C13-O15-H16	104.69	105.73

The maximum number of potentially active observable fundamentals of a non-liner molecule that contains N atoms is equal to (3n-6), apart from three translational and three rotational degrees of freedom [10]. 3HN2CA having 22 atoms with 60 Normal modes of vibrations which are distributed amongst the symmetry species as (3N-6)$_{vib}$=41A' (in-plane) + 19" (out-of-plane). The A' vibrations are totally symmetric and give rise to polarized Raman lines whereas A" vibrations are antisymmetric and give rise to depolarized Raman lines. Figs.2 and 3 shows the observed and calculated B3LYP/ccPVDZ and B3LYP/6-31+G(d)FT-IR and FT-Raman spectra of 3HN2CA , respectively.

The most optimized geometrical parameters (bond lengthand bond angle) were calculated by B3LYP/ccPVDZ and B3LYP/6-31+G(d)basis sets, which are depicted in Table 1.

Vibrational Assignments

The detailed vibrational analysis of fundamental modes of 3HN2CA along with the FT-IR and FT-Raman experimental frequencies and the unscaled and scaled vibrational frequencies using B3LYP/ccPVDZ and B3LYP/6-31+G(d)basis sets are presented in Table 2.

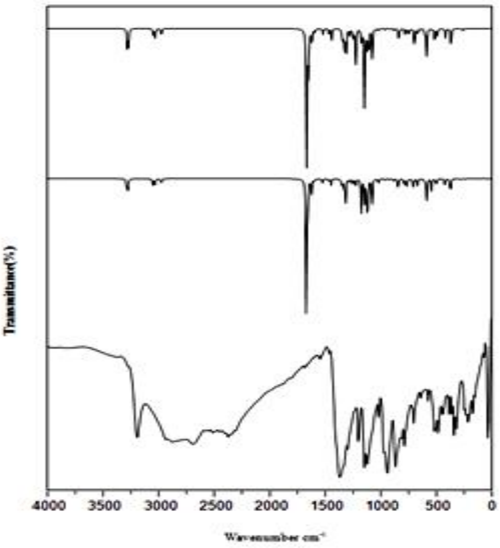

Fig.2 Observed and simulated FT-IR spectra of 3-hydroxynaphthalene-2-carboxylicacid

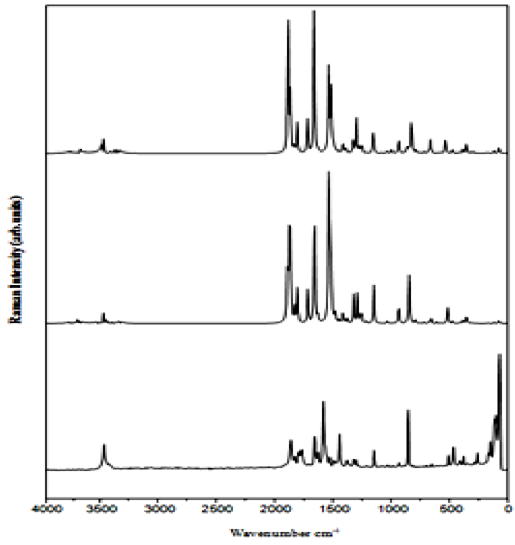

Fig. 3 Observed and simulated FT- Raman spectra of 3-hydroxynaphthalene-2-carboxylicacid

CH vibrations

The assignments of the carbon-hydrogen stretching are straight forward on the basis of the B3LYP/ ccPVDZ and B3LYP/6-31+G(d) predicted wavenumbers. The 3HN2CA molecule gives rise to six C–H stretching, six C–H in-plane bending and six C–H out-of-plane bending vibrations. Aromatic compounds commonly exhibit multiple weak bands in the region 3100-3000 cm^{-1} due to aromatic C-H stretching vibration [11]. The aromatic C–H stretching vibrations are observed in the region 3044 and 3005 cm^{-1} are in agreement with recorded FT-IR and FT-Raman spectrum at 3025 and 2980 cm^{-1}. The six C-H in-plane bending vibrations appears in the range 1000-1300 cm^{-1} in the substituted benzenes and the six out of plane bending vibrations occurs in the wave number range 750-1000 cm^{-1} are usually weak. The C-H in-plane bending vibrations are assigned at 1072,1015 and 955 cm^{-1} in infrared and 1073 and 1017cm^{-1} in Raman. The computed wave numbers 1125, 1109, 1076, 1019,983 and 959cm^{-1} are calculated by B3LYP/ccPVDZ method 1120, 1110,1073, 1016, 980 and 956 cm^{-1} by B3LYP/6- 31+G(d)method. The infrared bands are observed at 598, 582, 508, 496, 456cm^{-1} are assigned to C–H out-of-plane bending vibrations. The calculated values are found at595, 586, 540, 514, 490 and 473cm^{-1} by B3LYP, respectively, are assigned to C-H out-ofplane bending vibrations. These observed values of C-H vibrations of 3HN2CA are assigned within the characteristic region and is presented in Table 2.

Ring vibrations

In case of 3HN2CA, the carbon atoms coupled together in the hexagonal chain of benzene possesses six C-C stretching vibrations in the region of 1460–1150 cm^{-1}. According to the PED results, the ring C-C stretching modes are observed at 1599, 1515, 1466, 1441, 1351, 1281 and 1218 cm^{-1} in FT-IR and 1591, 1466, 1442, 1352, 1278 and 1220 cm^{-1} in FT-Raman for 3HN2CA. The in-plane and out-of-plane bending vibrations of benzene ring are generally observed below 1000 cm^{-1}[12] and these modes are not pure but they contributes drastically from other vibrations and are substituent-sensitive. In the title molecule, ring in-plane (δring) and out-of plane(γring) bending modes are affected to a great extent by the substituents and produce bands below 900 cm^{-1}. The scaled theoretical wavenumbers corresponding to ring vibrations are found to have a good correlation with their available experimental observations.

OH vibrations

The O–H stretching vibrations normally appear around 3600 cm^{-1} as in phenol [13]. For 3HN2CA, the band values observed at 3283cm^{-1} in infrared spectrum are ascribed to O–H stretching vibration. These values are below the expected value due to the nature and position of the substituents. The values found at 1170cm^{-1} and 677cm^{-1} are assigned to O–H in-plane and out-of-plane bending vibrations of 3HN2CA. These vibrations show good agreement with computed harmonic frequency as well as with recorded spectral data.

COOH vibrations

The vibrational assignments of carboxylic acid group of the title molecule have great deal of interest. The derivatives of carboxylic acids are best characterized by the carbonyl and hydroxyl groups. In particular, the presence of carbonyl group is most important in the infrared spectrum because of its strong intensity of absorption and high sensitivity toward relatively minor changes in its environment. Intra and intermolecular hydrogen bonding interactions affect the carbonyl absorptions in common organic compounds due to inductive, mesomeric, field and conjugation effects [14].

The characteristic infrared absorption wavenumber of C=O in acids are normally strong in intensity and are found in the region 1690–1800 cm−1 [15,16]. In the present study, the strong band at 1663 cm^{-1} in FT-IR is assigned to C=O stretching. The calculated value of this mode at B3LYP/6-31+G(d) method is found to be in consistent with the experimental data.

Table 2. Vibrational assignments of fundamental observed frequencies and calculated frequencies of 3-hydroxynaphthalene-2-carboxylicacid by B3LYP/ccPVDZ and B3LYP/6-31+G(d)

Mode No.	Symmetry species	Observed frequencies		Calculated frequencies				Vibrational assignments / (%)
		FT-IR	FT-Raman	Unscaled		Scaled		
				B3LYP/ ccPVDZ	B3LYP/ 6-31+G(d)	B3LYP/ ccPVDZ	B3LYP/ 6-31+G(d)	
1.	A’	3283		3763	3738	3282	3280	υOH(100)
2.	A’			3725	3706	3270	3268	υOH(100)
3.	A’		3063	3220	3229	3065	3067	υCH(99)
4.	A’	3044		3201	3209	3047	3045	υCH(99)
5.	A’		3025	3188	3196	3030	3026	υCH(96)
6.	A’	3005		3175	3184	3009	3006	υCH(95)
7.	A’		2980	3169	3178	2981	2980	υCH(95)
8.	A’			3152	3160	2973	2970	υCH(94)
9.	A’	1663		1819	1801	1668	1665	υC=O(83)
10.	A’		1648	1682	1679	1650	1650	υCC(86), δOH(12)
11.	A’		1616	1652	1650	1620	1617	υCC(87), δOH(9)
12.	A’	1599	1591	1617	1615	1596	1595	υCC(78), δOH (12)
13.	A’	1515		1562	1565	1520	1518	υCC(78), δOH(9), δCH (7)
14.	A’	1466	1466	1502	1515	1468	1466	υCC(69), δCH (17), δOH (6)
15.	A’	1441	1442	1484	1488	1440	1441	υCC(75), δOH (12), δCH (7)
16.	A’	1351	1352	1430	1426	1352	1353	υCC(78), δOH (14)
17.	A’			1407	1406	1341	1340	υCC (76), δCH (11), δOH(8)
18.	A’		1320	1376	1382	1326	1321	υCC (71), υOH(12)
19.	A’	1311		1365	1362	1310	1310	υC−O (75), δOH (14), δCH(6)
20.	A’	1281		1331	1331	1283	1280	υC−O (76)
21.	A’		1278	1286	1305	1280	1278	υCC(78), δOH (6)
22.	A’			1262	1271	1249	1250	υCC(74), δCH(12), δOH(7)
23.	A’	1218	1220	1208	1220	1226	1221	υCC(78), δOH (12)
24.	A’	1168	1170	1198	1205	1173	1170	δOH (81), δCH (11)
25.	A’	1146	1148	1184	1194	1147	1141	δOH (84), δCH(9)
26.	A’			1165	1179	1125	1120	δCH(78), δCO(17)
27.	A’			1145	1150	1109	1110	δCH(75), δCO (15)
28.	A’	1072	1073	1061	1056	1076	1073	δCH(64), δCO(15)
29.	A’	1015	1017	1042	1044	1019	1016	δCH(67),δC0(25)
30.	A’			1005	998	983	980	δCH(78), δOH(10)
31.	A’	955		979	974	959	956	δCH(77), δOH(12)
32.	A’		913	954	944	918	915	δC=O (73), γCC(21)
33.	A’	903		924	928	910	910	δR2$_{trigd,}$(65)
34.	A’	875	875	889	880	880	878	δR2$_{asym,}$(69)
35.	A’	843		846	846	837	838	δR2$_{sym,}$(68)
36.	A’	832	828	837	837	828	829	δCC(68), δOH(19)
37.	A’	789		808	798	784	785	δR1$_{trigd}$79), δCH(16)
38.	A’	767		785	763	764	765	δR1$_{asym}$ (79)
39.	A’	752	758	766	758	752	750	δCO(79),δCO(15),
40.	A’	730	727	759	757	732	734	δCO(73), δCH(13), υOH(12)
41.	A’			703	701	697	703	δR1$_{sym}$(79)
42.	A’’	664		687	677	668	665	γOH(65), δCO(18)
43.	A’’	636	625	637	639	633	636	γOH(65), δCO(21)
44.	A’’	598		602	604	595	597	γCH(79)
45.	A’’	582	580	587	590	586	581	γCH(77), υOH(14)
46.	A’’		538	559	559	540	539	γCH(69), γCO(19)
47.	A’’	508	511	558	553	514	509	γCH (65), γCO(19)
48.	A’’	496		489	485	490	494	γCH(51), γOH(34)
49.	A’’	456	453	448	448	473	457	γCH(51)
50.	A’’		415	439	432	418	418	γR2$_{trigd}$ (57), υOH(16)
51.	A’’		367	415	416	368	367	γR1$_{trigd}$ (53), υOH(21)
52.	A’’		339	389	389	340	340	γCC(53), υOH(13)
53.	A’’		310	337	337	314	312	γR2$_{asym}$(55)
54.	A’’		275	306	304	280	276	γR2$_{sym}$(49), υCO(53)
55.	A’’		255	305	303	259	236	γC=O(48), υOH(23)
56.	A’’		233	241	239	240	235	γCO(48)
57.	A’’		153	180	179	155	152	γCO(49), γOH(33)
58.	A’’		104	122	121	106	105	γRing Butterfly(59)
59.	A’’		66	86	85	67	67	γR1$_{asym}$ (47), γCH(21)
60.	A’’			38	22	30	30	γR1$_{sym}$ (44)

A’: In-plane; A”: out-of-plane; sym: symmetric stretching; asym: asymmetric stretching; υ:stretching;δ: in-plane bending; γ: out-of-plane bending; t: torsion; wagg: wagging; sciss:scissoring; τ: twisting; sb: symmetric bonding; ipb: in- plane-bending; opb: out-plane-bending; ipr:in-plane-rocking;opr: out-plane-r.

A band related to C–O stretching mode of carboxylic acid group is highly coupled with the vibrations of adjacent groups or atoms. Hence the wave number region for the existence of C–O is based on the nature of the nearby substitution. In the title molecule, the band at1311 and 1281cm^{-1} in FT-IR are assigned to C–O stretching mode. The C–O stretching mode normally appears in the frequency region 1200-1300 cm^{-1}. In the present study, the assignment this mode is somewhat lower than that of the literature [17].The O-H stretching vibrations are characterized by a very broad band appearing in the region 3400–3600 cm^{-1} [15]. In the present study, the OH band observed at3063cm^{-1} in FT-Raman spectrum. The scaled theoretical wavenumbers of C–O and O–H stretching modes at B3LYP/6-31+G(d) in the title molecule are matched well with the experimental value as well as the similar kind of molecules. In the case of 3HN2CA, the in-plane and out-of-plane bending vibrations are assigned to the modes are detailed in table. The predicted wave numbers related to these modes are found to be in agreement with their experimental observations.

Natural bond orbital (NBO) analysis

Natural bond orbital (NBO) method encompasses a suite of algorithms that enable fundamental bonding concepts to be extracted from density functional theory (DFT) computation. Natural bond orbital analysis originated as a technique for studying hybridization and covalence effects in polyatomic wave functions based on local block Eigen vectors of the one-particle density matrix. NBOs would correspond closely to the picture of localized bonds and lone pairs as basic units of molecular structure. The atomic charges of 3HN2CA calculated by NBO analysis using the B3LYP/6-3+G(d) method are presented in Table 3. Among the ring carbon atoms C1 of 3HN2CA have positive charges in B3LYP method. The positive charge on C1 is due to the attachment of highly electronegative hydroxyl to it. In 3HN2CA compound carbon attached with the carboxyl group has negative NBO charge. This is due to the electron withdrawing nature of the carboxyl group by means of resonance.

Donor–acceptor interactions: perturbation theory energy analysis

NBO analyses of molecule illustrate the deciphering of the molecular wave function in terms Lewis structures, charge, bond order, bond type, hybridization, resonance, donor–acceptor interactions, etc. The localized orbitals in the Lewis structure of 3HN2CA can interact strongly. These interactions can strengthen and weaken bonds. A lone pair donor → antibonding acceptor orbital interaction will weaken the bond associated with the anti-bonding orbital. Conversely, an interaction with a bonding pair will strengthen the bond. Strong electron delocalization in the Lewis structure also shows up as donor–acceptor interactions. This calculation is done by examining all possible interactions between ‘filled’ (donor) Lewis-type NBOs and ‘empty’ (acceptor) non-Lewis NBOs, and estimating their energetic importance by second order perturbation theory.

The NBO method demonstrates the bonding concepts like atomic charge, Lewis structure, bond type, hybridization, bond order, and charge transfer and resonance possibility. Natural bond orbital (NBO) analysis is a useful tool for understanding delocalization of electron density from occupied Lewis-type (donor) NBOs to properly unoccupied non-Lewis type (acceptor) NBOs within the molecule. The stabilization of orbital interaction is proportional to the energy difference between interacting orbitals. Therefore, the interaction having strongest stabilization takes place between effective donors and effective acceptors. This bonding, anti-bonding interaction can be quantitatively described in terms of the NBO approach that is expressed by means of second-order perturbation interaction energy E$^{(2)}$[18]. This energy represents the estimate of the off-diagonal NBO Fock matrix element. The stabilization energy E$^{(2)}$ associated with i (donor)→ j(acceptor) delocalization is estimated from the second-order perturbation approach as given below

$$E^{(2)} = q_i \frac{F^2(i, j)}{\varepsilon_j - \varepsilon_i} .$$

Where qi is the donor orbital occupancy, εi and εj are diagonal elements (orbital energies) and F(i,j) is the off-diagonal Fock matrix element.

The second order perturbation analyses of Fock matrix of 3HN2CA are summarized in Table 4. The Fock matrix analysis yields different types of donor–acceptor interactions and their stabilization energy. All lone pair–bond pair interactions and only bond pair–bond pair interactions with stabilization energies are listed in Table 4. In 3HN2CA molecule, the lone pair donor orbital, LPO15 → π*C13-O14 interaction between the O15 lone pair and the C13-O14 antibonding orbital is seen to give a strong stabilization, 43.77 kJ mol^{-1}and LP14 → π*C13-O15 interaction has the stabilization energy of 31.53 kJ mol^{-1}. These stabilization energies of lone pair–bond pair and bond pair–bond pair interactions are give more stabilization than other interactions. The π electron cloud movement from donor to acceptor can make the molecule highly polarized and the 3HN2CA is present and it must be responsible for the NLO properties.

The NBO analysis also describes the bonding in terms of the natural hybrid orbital LPO15, which occupy a higher energy orbital with considerable p-character (58.85%) and low occupation number (1.97607 a.u.) and the other LPO14 occupy a lower energy orbital with p-character (38.74%) and high occupation number (1.97726 a.u.). Thus, a close to pure p-type lone pair participates in the electron donation to the σ* C2-C1, and σ*C2-C3 orbital for LPO14→σ*C-C interaction in the compound. The other natural hybrid orbital interactions are presented in Table 4

Frontier molecular orbital’s (FMOs) and atomic charges

The most important orbital’s in molecule is the frontier molecular orbital’s, called highest occupied molecular orbital (HOMO) and lowest unoccupied molecular orbital (LUMO). These orbitals determine the way the molecule interacts with other species. The frontier orbital gap helps to characterize the chemical reactivity and kinetic stability of the molecule. A molecule with a small frontier orbital gap is more polarizable and is generally associated with a high chemical reactivity, low kinetic stability and is also termed as soft molecule [19]. The low values of frontier orbital gap in 3HN2CA make it more reactive and less stable. The HOMO is the orbital that primarily acts as an electron donor and the LUMO is the orbital that largely acts as the electron acceptor. The 3D plot of the frontier orbital’s HOMO and LUMO for 3HN2CA molecule are shown in Fig. 4. The positive phase is red and the negative one is green (For interpretation of the references to color in this text, the reader is referred to the web version of the article). Many organic molecules, containing conjugated p electrons are characterized by large values of molecular first hyperpolarizabilities, were analyzed by means of vibrational spectroscopy [20, 21].

In most cases, even in the absence of inversion symmetry, the strongest band in the FT-Raman spectrum is weak in the FT-IR spectrum vice versa. But the intra-molecular charge transfer from the donor to acceptor group through a single-double bond conjugated path can induce large variations of both the molecular dipole moment and the molecular polarizability, making FTIR and FT-Raman activity strong at the same time. The experimental spectroscopic behavior described above is well accounted by ab initio calculations in p conjugated systems that predict exceptionally large Raman and IR intensities for the same normal modes [21]. It is also observed in our title molecule the bands in FTIR spectrum have their counterparts in FT-Raman shows that the relative intensities in FTIR and FT- Raman spectra are comparable resulting from the electron cloud movement through π conjugated frame work from the electron donor to electron acceptor groups. The analysis of the wave function indicates that the electron absorption corresponds to the transition from the ground to the first excited state and is mainly described by one-electron excitation from the highest occupied molecular orbital (HOMO) to the lowest unoccupied molecular orbital (LUMO). The HOMO of π nature, (i.e., benzene ring) is delocalized over the C–C bond. By contrast, LUMO is located over hydroxyl, and oxygen atoms of carboxylic acid group. It can be seen from the Fig. 4 that, the HOMO is distributed in ring and hydroxyl group of title molecule. The LUMO in C2–C13 and O14 of carboxylic acid group are found to spread over the ring. All the HOMO and LUMO have nodes. The nodes in each HOMO and LUMO are placed symmetrically.

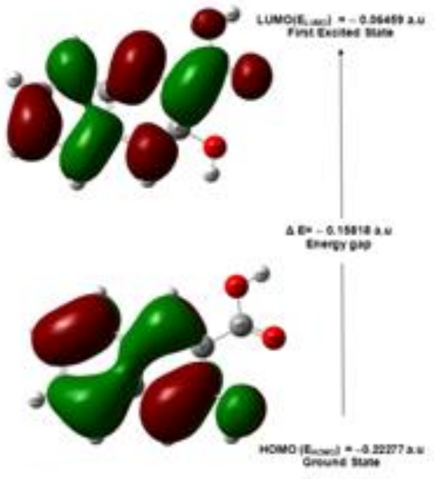

Fig. 4. The atomic orbital composition of the molecular orbital for 3-hydroxy naphthalene-2-carboxylicacid

The energy gap of HOMO-LUMO explains the eventual charge transfer interaction within the molecule, which influences the NLO activity of the molecule. As the energy gap between the LUMO and HOMO decreases, it is easier for the electrons of the HOMO to be excited. The higher the energy of HOMO, the easier it is for HOMO to donate electrons whereas it is easier for LUMO to accept electrons when the energy of LUMO is low. The energy values of HOMO and LUMO levels are computed to be -0.22277 a.u. and -0.06459 a.u., respectively, and the energy difference is 0.15818 a.u.

The calculation of atomic charges plays a key role in the application of quantum mechanical calculation to describe the electronic characteristics of molecular systems [22]. A comparative study of the NBO and Mullikan atomic charge distributions in 3-Hydroxy naphthalene-2-carboxylicacid.determined on the basis of quantum mechanical method with B3LYP method is presented in Table 3.

Both Mullikan's atomic net charges [23–25] and the natural NBO/NPA atomic charges were calculated. The results are listed in Table 3. Regarding the molecular symmetries only the charges of 22 atoms are listed for title molecule.

The comparison between Mullikan's net charges and the atomic natural one is not an easy task since the theoretical background of the two methods was very different. Looking at the results there are surprising differences between the Mullikan's and the NBO charges. All of the NBO charges have the positive sign for C2 atom and negative sign for C1 atom on the B3LYP method, whilst the Mullikan's values for the C1 and C2 atoms are different in sign as compared to these values for the method.

The definition of Mullikan's charges is based on population analysis. The Mullikan population analysis provides a partitioning of either the total charge density or an orbital density. The number of electrons in molecule (N) is the integral of the charge density over the space. N is partitioned for all atoms considering also the overlap population. According to the theory the overlap population of atoms A and B is divided between the two atoms in half-to-half ratio. This is one weak point of the theory. The other weak point is its strong dependence on the basis set applied. The Mullikan's atomic net charges are presented in Table 3.

Table 3. The charge distribution calculated by the Mulliken and natural bond orbital (NBO) methods using DFT/B3LYP/6-31+G(d)of 3-hydroxy naphthalene -2-carboxylicacid molecule.

Atoms	Atomic charges (Mulliken)	Natural charges (NBO)
C1	0.081559	-0.14292
C2	-0.240446	0.19822
C3	-0.232787	0.33682
C4	-0.364473	-0.28109
C5	-0.332664	-0.21869
C6	-0.283737	-0.21991
C7	-0.411934	-0.24628
C8	-0.161961	-0.19326
C9	-0.043661	-0.08203
C10	0.373122	-0.03455
O11	-0.635581	-0.68910
H12	0.501837	0.50025
C13	1.207370	0.80452
O14	-0.460741	-0.58720
O15	-0.648076	-0.74069
H16	0.518645	0.52410
H17	0.167664	0.23539
H18	0.183988	0.23529
H19	0.183580	0.24338
H20	0.183529	0.24323
H21	0.189254	0.24156
H22	0.225713	0.26539

Molecular electrostatic potentials (MEPs)

Molecular electrostatic potential (ESP) at a point in the space around a molecule gives an indication of the net electrostatic effect produced at that point by the total charge distribution (electron + nuclei) of the molecule and correlates with dipole moments, electronegativity, partial charges and chemical reactivity of the molecules. It provides a visual method to understand the relative polarity of the molecule. An electron density isosurface mapped with electrostatic potential surface depicts the size, shape, charge density and site of chemical reactivity of the molecules. The different values of the electrostatic potential represented by different colors; red represents the regions of the most negative electrostatic potential, blue represents the regions of the most positive electrostatic potential and green represents the region of zero potential. Potential increases in the order red < orange < yellow < green < blue. Such mapped electrostatic potential surfaces have been plotted for title molecule in B3LYP/6-31+G(d) basis set using the computer software Gauss view. Projections of these surfaces along the molecular plane and a perpendicular plane are given in Fig. 5. This figure provides a visual representation of the chemically active sites and comparative reactivity of atoms. It may see that, in both methods, a region of zero potential envelopes the p-system of the aromatic rings, leaving a more electrophilic region in the plane of hydrogen atoms in 3HN2CA molecule [26].

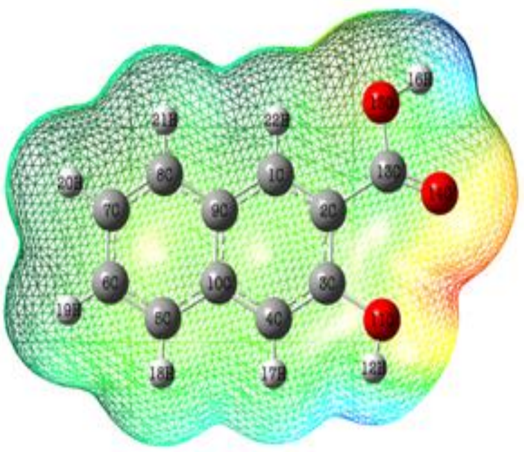

Fig 5. DFT (B3LYP)/6-31+G(D) calculated 3D molecular electrostatic potential of 3-hydroxynaphthalene-2-carboxylicacid

Table 4. Second-order perturbation theory analysis of Fock matrix in NBO basic corresponding to the intra molecular bonds of 3-hydroxynaphthalene -2-carboxylicacid.

Donor(i)	ED(i) (e)	Acceptor (j)	ED(j) (e)	$^{a}E^{(2)}$ (kJ mol^{-1})	^{b}E(j) – E(i) (a.u.)	^{c}F(i,j) (a.u.)
σ(C_1–C_9)	1.96540	σ*(C_2–C_{13})	0.07235	3.52	1.05	0.069
σ(C_1–H_{22})	1.97727	σ*(C_2–C_3)	0.02870	4.67	1.07	0.063
σ(C_2–C_{13})	1.97234	σ*(C_{15}–H_{16})	0.01400	3.05	1.06	0.051
σ(C_3–O_{11})	1.99357	σ*(C_4–C_{10})	0.02076	1.81	1.37	0.045
σ(C_4–C_{10})	1.97081	σ*(C_3–O_{11})	0.02389	4.55	0.96	0.059
σ(C_5–C_9)	1.97575	σ*(C_9–C_{10})	0.03104	3.01	1.23	0.055
σ(C_8–C_9)	1.97576	σ*(C_9–C_{10})	0.03104	3.09	1.23	0.055
σ(O_{11}–H_{12})	1.98980	σ*(C_2–C_3)	0.02870	4.51	1.28	0.068
σ(C_{13}–O_{14})	1.99697	σ*(C_1–C_2)	0.01512	3.36	0.40	0.035
σ(C_{13}–O_{15})	1.99609	σ*(C_2–C_3)	0.02870	1.16	1.46	0.037
σ(O_{15}–H_{16})	1.98789	σ*(C_2–C_{13})	0.07235	4.23	1.13	0.063
LP(1)C_9	1.02275	σ*(C_1–C_2)	0.01512	65.51	0.14	0.104
LP(1)O_{14}	1.97726	σ*(C_2–C_{13})	0.07235	3.06	1.07	0.052
LP(1)O_{15}	1.97607	σ*(C_{13}–O_{14})	0.23900	6.65	1.16	0.079
LP(2)O_{14}	1.85108	π*(C_{13}–C_{15})	0.09304	31.53	0.60	0.124
LP(2)O_{15}	1.83281	π*(C_{13}–O_{14})	0.23900	43.77	0.34	0.110

Thermodynamic properties

On the basis of vibrational analysis, the statically thermodynamic functions: heat capacity (Cp), enthalpy changes (ΔH), Gibb's free energy (Δ) and entropy (S^0m) for the title molecule were obtained from the theoretical harmonic frequencies and listed in Table 5. From the Table 5, it can be observed that these thermodynamic functions are increasing with temperature ranging from 100 to 1000 K due to the fact that the molecular vibrational intensities increase with temperature. The correlation equations between heat capacity, Gibb's free energy, entropy, enthalpy changes and temperatures were fitted by quadratic formulas and the corresponding fitting factors (R2) for these thermodynamic properties are 0.999, 0.999, 1.000 and 0.999, respectively. The corresponding fitting equations are as follows and the correlation graphics of those shown in Fig. 6

$$\left(Cp^{0}\right) = -0.015 + 17.75T - 0.790T^{2}(R^{2} = 0.999)$$

$$(S^{0}) = 57.16 + 18.61T - 0.224T^{2}(R^{2} = 1)$$

$$(H - E/T) = 3.057 + 8.845T + 0.416T^{2}(R^{2} = 0.999)$$

$$(G - E/T) = -54.10 - 9.772T + 0.191T^{2}(R^{2}0.999)$$

All the thermodynamic data supply helpful information for the further study on the 1HN2CA. They can be used to compute the other thermodynamic energies according to relationships of thermodynamic functions and estimate directions of chemical reactions according to the second law of thermodynamics in thermo chemical field. Notice: all thermodynamic calculations were done in gas phase and they could not be used in solution.

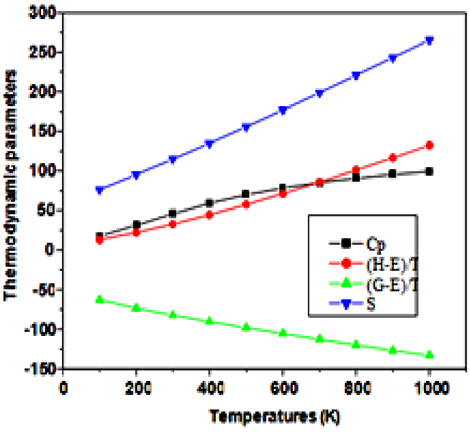

Fig. 6 Correlation graphic of thermodynamic parameters and temperature for 3-hydroxynaphthalene 2-carboxylicacid

Table 5. Thermodynamic functions of 3-hydroxy naphthalene - 2 - carboxylicacid

Temp (K)	Cp (Cal Mol^{-1}K^{-1})	(H-E)/T (Cal Mol^{-1}K^{-1})	(G-E)/T (Cal Mol^{-1}K^{-1})	S (Cal Mol^{-1}K^{-1})
100	17.55	13.11	-63.05	76.16
200	31.22	22.05	-73.42	95.47
300	45.78	32.69	-82.11	114.80
400	58.93	44.62	-90.27	134.89
500	69.76	57.58	-98.10	155.68
600	78.39	71.38	-105.65	177.03
700	85.25	85.89	-112.91	198.79
800	90.78	100.97	-119.87	220.84
900	95.33	116.54	-126.55	243.09
1000	99.11	132.51	-132.96	265.47

In addition to the vibrational assignments, several thermodynamic parameters, rotational constants, and dipole moment have been presented in Table 6. The self consistent field (SCF) energy, zero point vibrational energies (ZPVEs), rotational constants and entropy $S_{vib}(T)$ are calculated to the extent of accuracy and variations in the ZPVEs seem to be insignificant [27]. Dipole moment reflects the molecular charge distribution and is given as a vector in three dimensions. Therefore, it can be used as descriptor to depict the charge movement across the molecule. Direction of the dipole moment vector in a molecule depends on the centers of positive and negative charges. Dipole moments are strictly determined for neutral molecules. For charged systems, its value depends on the choice of origin and molecular orientation.

Table 6. Thermodynamic functions of 3-hydroxynaphthalene -2-carboxylicacid.

Parameter	B3LYP/ccPVDZ
Self consistent field energy	-649.7032 a.u
Zero point vibrational energy	104.37660(kcal/mol)
Rotational constants	1.54855GHz
	0.45714 GHz
	0.35295 GHz
Entropy	104.335 cal/mol K
Specific heat capacity at constant volume	43.538 cal/mol K
Translational energy	41.601cal/mol K
Rotational energy	31.532 cal/mol K
Vibrational energy	31.202 cal/mol K

Conclusions

The present investigation thoroughly analyzed the HOMO-LUMO analyses, NBO and the vibrational spectra, and both infrared and Raman of 3- hydroxynaphthalene-2-carboxylicacid. Based on theoretically calculated energy difference. All the vibrational bands observed in the FT-IR and FT-Raman spectra of these compounds are assigned to the various modes of vibration, and most of the modes have wavenumbers in the expected range. The complete vibrational assignments of wavenumbers are made on the basis of potential energy distribution (PED). The scaled B3LYP methods with ccPVDZ and 6-31+G(d) basis sets. results are the best over the other methods. The electrostatic potential surfaces (ESP) together with complete analysis of the vibrational spectra, both IR and Raman electronic spectra, helps us to identify the structural and symmetric properties of 3HN2CA The excellent agreement of the calculated and observed vibrational spectra reveals the advantages of higher basis set for quantum chemical calculations. NBO analysis provides an efficient method for studying inter and intra molecular interactions in molecular system. The stabilization energy has been calculated from second-order perturbation theory. Natural bond orbital analysis shows that the differences in interaction of energies are due to the substitution of COOH, and OH groups, respectively. The thermodynamic functions (heat capacity, internal heat energy, Gibbs energy and entropy), from spectroscopic data by statistical methods were obtained for the range of temperature 100-1000 K. The gradients of Cp, $S_{m,}$(H-E), and vibrational intensity increases with increase of temperature.

References

[1] Milligan, D. E.; Jacox, M. E.. "Infrared Spectrum and Structure of Intermediates in Reaction of OH with CO". Journal of Chemical Physics 54 (3) 927–942.

[2] Jeevarajan, A. S.; Carmichael, I.; Fessenden, R. W. "ESR Measurement of the pKa of Carboxyl Radical and Ab Initio Calculation of the C-13 Hyperfine Constant". Journal of Physical Chemistry 94 (4) (1990) 1372–1376.

[3] Morrison, R.T. and Boyd, R.N. Organic Chemistry, 6th ed. (1992).

[4] M.J. Frisch, G.W. Trucks, H.B. Schlegal, G.E. Scuseria, M.A. Robb, et al., Gaussian 09, Revision A. 02, Gaussian Inc., Wallingford, CT, 2009.

[5] A. Frisch, A.B. Niesen, A.J. Holder, Gauses View Users Manual, Gaussian Inc.,2008.

[6] A.E. Reed, F. Weinhold, J. Chem. Phys. 83 (1985) 1736–1740.

[7] M. Snehalatha, C. Ravi Kumar, I. Hubert Joe, V.S. Jaya Kumar, J. Raman Spectrosc. 40 (2009) 1121–1126.

[8] I. Hubert Joe, I. Kostova, C. Ravi Kumar, M. Amalanathan, S.C. Pinzaru, J. Raman Spectrosc. 40 (2009) 1033–1038.

[9] A.E. Ledesma, J. Zinczuk, A. Ben Altabef, J.J. Lopez Gonzalez, S.A. Brandan, J Raman Spectrosc. 40 (2009) 1004–1010.

[10] M. Silverstein, G. Clayton Basseler, C. Morill, Spectrometric Identification of Organic Compound, Wiley, New York, 1981.2560.

[11] M.K. Subramanian, P.M. Anbarsan, S. Manimegalai, J. Raman Spectrosc 40(2009) 1657−1663.

[12] N.P. Roeges, A Guide to the Complete Interpretation of Infrared Spectra of Organic Structures, Wiley, New York, 1994.

[13] H. Lampert, W. Mikenda, A. Karpten, J. Phys. Chem. 101 (1997) 2254. 2263.

[14] V. Krishnakumar, R. Mathamal, J. Raman Spectrosc. 40 (2009) 264–271.

[15] M. Karabacak, M. Kurt, J. Mol. Struct. 919 (2009) 215–222.

[16] M. Silverstein, G. Clayton Basseler, C. Morill, Spectrometric Identification of Organic Compounds, Wiley, New York, 1981.

[17] P.D.S. Babu, S. Periyandi, S. Ramalingam, Spectrochim. Acta A 78 (2011) 1321–1328.

[18] J.P. Foster, F. Weinhold, J. Am. Chem. Soc. 102 (1980) 7211–7218.

[19] B.J. Powell, T. Baruah, N. Bernstein, K. Brake, R.H. McKenzie, P. Meredith, M.R. Pederson, J. Chem. Phys. 120 (2004) 8608–8615.

[20] Y. Ataly, D. Avci, A. Basoglu, J. Struct. Chem. 19 (2008) 239–246.

[21] T. Vijayakumar, I. Hubert Joe, C.P.R. Nair, V.S. Jayakumar, J. Chem. Phys. 343 (2008) 83–99.

[22] Xavier Assfeld, J.L. Rivail, Chem. Phys. Lett. 263 (1996) 100–106.

[23] R.S. Mullikan, J. Chem. Phys. 23 (1955) 1833–1841.

[24] A.E. Reed, F.J. Weinhold, L.A. Curtiss, Chem. Rev. 88 (1988) 899–926.

[25] R.G. Parr, L.V. Szentpaly, S.J. Liu, Am. Chem. Soc. 121 (1999) 1922–1924.

[26] V.P. Gupta, A. Sharma, V. Virdi, V.J. Ram, Spectrochim. Acta, Part A 64 (2006) 57–67.

[27] P.B. Nagabalasubramanian, S. Periyandi, S. Mohan, Spectrochim. Acta, Part A 77 (2010) 150–159.